

PAPER • OPEN ACCESS

Terrain Estimation with Least Squares and Virtual Model Control for Quadruped Robots

To cite this article: Haipeng Qin *et al* 2022 *J. Phys.: Conf. Ser.* **2203** 012005

View the [article online](#) for updates and enhancements.

You may also like

- [Optimal planar leg geometry in robots and crabs for idealized rocky terrain](#)

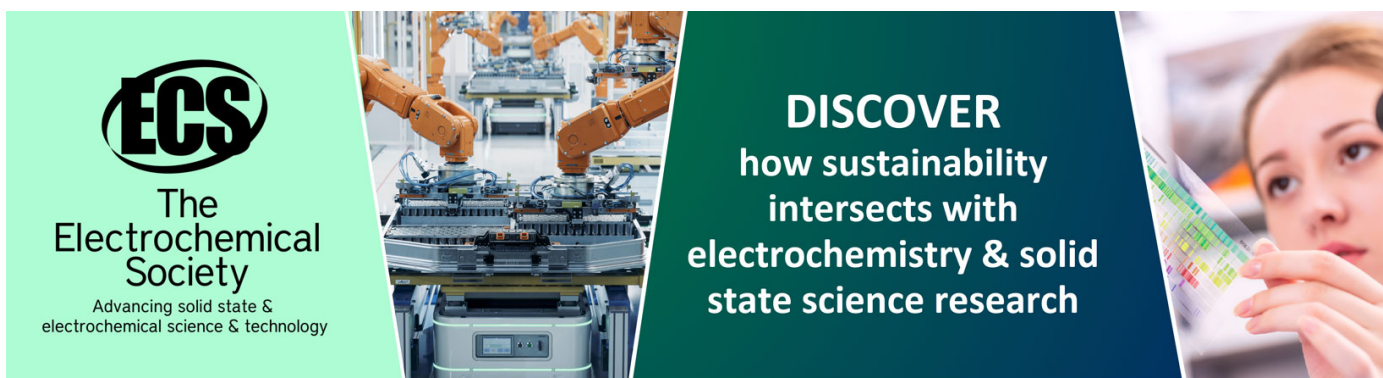
Yang Chen, Glenna Clifton, Nicole M Graf et al.

- [An insect-scale robot reveals the effects of different body dynamics regimes during open-loop running in feature-laden terrain](#)

Perrin E Schiebel, Jennifer Shum, Henry Cerbone et al.

- [Bio-inspired robotic dog paddling: kinematic and hydro-dynamic analysis](#)

Yunqian Li, Frank Fish, Yonghua Chen et al.



ECS
The
Electrochemical
Society
Advancing solid state &
electrochemical science & technology

DISCOVER
how sustainability
intersects with
electrochemistry & solid
state science research

Terrain Estimation with Least Squares and Virtual Model Control for Quadruped Robots

Haipeng Qin¹, Yaguang Zhu^{1,2*}, Yaqiang Zhang¹, Qibin Wei¹

¹Key Laboratory of Road Construction Technology and Equipment of MOE, Chang'an University, Xi'an 710064, China

²State Key Laboratory of Fluid Power and Mechatronic Systems, Zhejiang University, Hangzhou 310027, China

*Email: Yaguang Zhu(e-mail:zhuyaguang@chd.edu.cn)

Abstract. In this paper, a method to estimate the terrain based on footholds and least-squares is presented to make quadrupedal locomotion stable on the sloped terrains, with joint encoders, force sensors and inertial measurement unit (IMU) instead of visual sensors. This method which is tested successfully in simulation can predict two types of terrain, one for adjusting the robot pose and the other for adjusting the trajectory of swing phase. And to make full use of these new capabilities, general balance and locomotion controller is presented. The virtual model controller is embedded into architecture and it allows the robot to handle unexpected terrain. The quadrupedal locomotion in terrain with different inclination prove the robustness of this method.

1. Introduction

In nature, quadruped animals are common due to their agility and strong adaptability to the complex terrain. With the advantages of legged structure and the favour of roboticists, the quadruped robot has become one of the biggest hotspots in the field of biomimetic robot research. BigDog [1] have demonstrated dynamic running in outdoor environments with great robustness. To improve the ability to adapt unknown and complex terrain, some scholars take the terrain recognition [2] into consideration. HyQ [3] accomplished better interaction between feet and ground with off-line maps created by Alexander with Kinect sensors and the foot-force feedback [4]. The ways of recognizing terrain based on perceptual sensors [5], laser scanners [6] and binocular cameras [7], make the terrain estimation more precise but equipment cost higher and computation more complex. This paper presents a method based on the least-squares and optimization to recognize terrains without relying on vision.

The paper is organized as follows: Section 2 describes the mechanical structure of quadruped robot. The contributions about terrain estimation are discussed in Section 3 and the virtual model controller and simulation are detailed in Section 4 and 5 respectively. Finally, we draw the conclusions in Section 6.

2. The Model of the Quadruped

2.1. Mechanical Structure

The quadrupedal platform (Figure 1) consists of a main body and four legs with each leg owning three degrees of freedom. The robot's parameter shows as follows: the body length 590 mm, width 200 mm, and the thigh length 190 mm, the calf length 300 mm. The robot's body and legs are made of light-weight aluminium alloy material, which weight totally 40 kg or so. And Figure 2 shows our prototype,



every joint is driven by the motor. For the purpose of minimizing limb mass and inertia, the hip and knee motors are located coaxially at the hip joint, and the knee joint is driven by the torque transmitted from the motor through a link. And Joint encoders, IMU sensor and force sensors are equipped so that the motion parameters can be known.

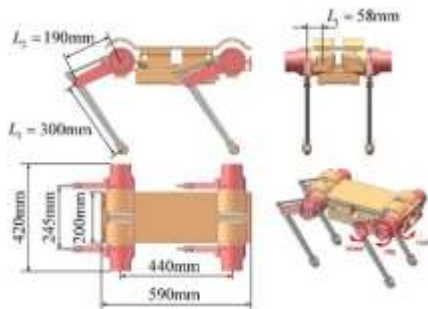


Figure 1. The quadruped platform.

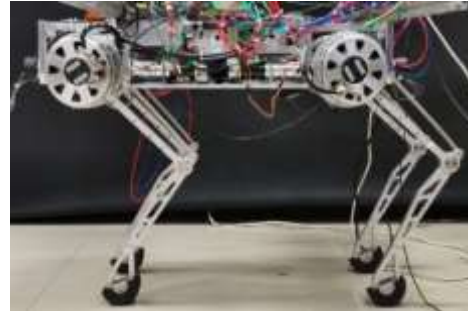


Figure 2. The quadruped prototype platform.

2.2. Kinematics Modelling

In order to express the spatial relationship between each part of the robot, a torso frame $\{B\}$ is established. To express the pose and position of the base of the robot, a world frame $\{W\}$ is established, in which the axis's pointing determines as same as frame $\{B\}$. Each leg has a root frame $\{R_i\}, i = \{LF, LH, RF, RH\}$, whose origin is set at the intersection of the root joint axis and the hip joint axis, and whose axis direction is consistent with $\{B\}$.

Kinematics analysis is done on only one of these legs because of the same structure among them. The model of leg is shown as Figure 1, including the root link measured L_1 , the thigh link measured L_2 , and the calf link measured L_3 . Through geometric analysis, the position of foot tip in $\{W\}$:

$${}^W P_i = {}^W P_c + {}^W R {}^B P_i \quad (1)$$

where ${}^W P_c$ represents the centroid position of the base, ${}^B P_i$ represents the foot position in the frame $\{B\}$ and the following variables described in $\{W\}$ will ignore the superscript by default.

3. The Terrain Estimation

3.1. Terrain for Base Pose Adjustment

As the ground is not always a flat plane, adaption to the sloped terrain needs to be taken into consideration. Robots adjust their pose [8] and trajectory according to the terrain's inclination. So, it is important to obtain the accurate information about the terrain. In the research of paper [9-10], a terrain-estimation approach has been proposed corresponding to the diagonal gait. This method estimates the macro-terrain as a plane in 3D space utilizing the most recent positions of the feet in contact with environment in $\{W\}$ expressed as $P_i = [x_i, y_i, z_i]^T, i = \{LF, LH, RF, RH\}$. The equation to estimate terrain is:

$$Z = b_0 + b_1 x + b_2 y \quad (2)$$

Terrain estimation [11] is applied to the current ground. There is several contact positions available for each leg, but earlier position means larger error, so the latest positions of the feet are adopted. Abbreviate (2) as $Wb = z$. With the matrix $W^{4 \times 3}$ and $Z^{4 \times 1}$ already known, the terrain plane can be obtained if $b^{3 \times 1}$ is solved.

If these four contact positions are not on the same plane, (3) can be solved by the least-squares and fit a plane closest to the real terrain.

$$W^T (Wb) = W^T z, b = (W^T W)^+ W^T z \quad (3)$$

where the superscript \dagger indicates pseudo-inverse matrix.

3.2. Terrain for Trajectory Planning

When robot stands on slopes, if the trajectory keeps still as standing on the flat ground, Figure 3 for example, the fore-feet on slopes will touch-down early, while the hind-feet on the flat ground later, which will lead to a large contact force peak [12]. To enhance the motion robustness, in this paper, terrain estimation is computed for each leg.

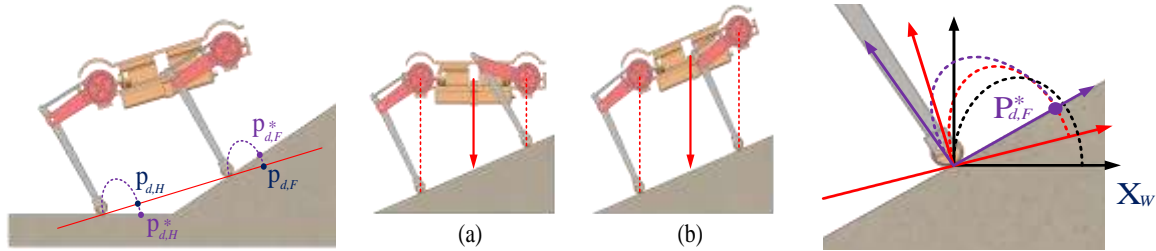


Figure 3. Robots on slopes. **Figure 4.** Adaption of the terrain. **Figure 5.** Adaption of the swing trajectory.

The collection of the previous contact positions $S = \{P_i | P_i = [x_i, y_i, z_i]^T, i = 1, 2, \dots, n, n > 4\}$, consists of the latest contact positions in frame $\{W\}$. We choose four proper positions from collection S , according to:

$$\begin{aligned} \min J &= \sum_{i=1}^n \lambda_i \|p_i - p_d\| \\ \text{s.t. } \sum_{i=1}^n \lambda_i &= 4, \lambda_i \in \{0, 1\}, \lambda_i + \lambda_j \leq 1, i, j = 1, 2, \dots, n, \forall i, j \in \{p_i \approx p_j\} \\ \lambda_i + \lambda_j + \lambda_k + \lambda_l &\leq 3, \forall i, j, k, l \in \left\{ \frac{\vec{P_i P_j}}{\|P_i P_j\|} \approx \frac{\vec{P_i P_k}}{\|P_i P_k\|} \approx \frac{\vec{P_i P_l}}{\|P_i P_l\|} \right\}, 1 \leq i < j < k < l \leq n \end{aligned} \quad (4)$$

where λ_i is the flag for decision, $\lambda_i = 1$ means point p_i is chosen, $\lambda_i = 0$ means not.

After considering the constraints above, an optimal method is used to find four positions of feet closest to the desired. The case that positions of four feet are collinear should be avoided, otherwise there will be no plane fitted.

3.3. Adaption of the Terrain

Quadrupedal locomotion on slopes (Figure 4(a)) makes the fore-legs compressed excessively if the body still maintains the horizontal posture, which will make the motion break the joint's limits then lead to the target position unrealizable. So, this paper adapts the torso's orientation aligned to the slope, such as Figure 4(b). When the stance feet are set directly below the hips, the contact force applied to each leg is balanced, which makes it easier to move on slopes.

According to Figure 3, the swing trajectory [13] also needs to be adapted to the terrain to maintain the stability of quadrupedal locomotion. To this end, the swing trajectory should be aligned to the estimated terrain around the foot tips, shown as Figure 5.

4. Basic Balance Control

4.1. The Model of the Stance Phase

The Balance Control enforces PD control on the centre of mass and body orientation, while also ensuring that foot forces satisfy friction constraints. The PD control law is given by:

$$\begin{bmatrix} \dot{v}_{c,d} \\ \dot{w}_{b,d} \end{bmatrix} = \begin{bmatrix} K_{cp}(p_{c,d} - p_c) + K_{cd}(v_{c,d} - v_c) \\ K_{bp}e({}^W R_d {}^W R_B^T) + K_{bd}(w_{b,d} - w_b) \end{bmatrix} \quad (5)$$

where K_{cp} and K_{cd} are the proportional and derivative gains about the linear acceleration of the body, K_{bp} and K_{bd} about the angular acceleration, which all are diagonal matrix.

If the forces applied to the feet is directly acting on the torso, the relationship between the feet force and the linear acceleration \dot{v}_c and angular acceleration \dot{w}_b of the *CoF* is:

$$\begin{bmatrix} I & I & I & I \\ {}^W_B P_1 & {}^W_B P_2 & {}^W_B P_3 & {}^W_B P_4 \end{bmatrix} \mathbf{f} = \begin{bmatrix} m(\dot{v}_c - g) \\ I_G \dot{w}_b \end{bmatrix} \quad (6)$$

where $I^{3 \times 3}$ is the unit matrix, $I_G^{3 \times 3}$ is the inertia of the torso, $g = [0, 0, 9.8]^T$. Abbreviate (6) as $Af = d$, where $A^{6 \times 12}$ provides six constraints, $f^{12 \times 1}$ is the twelve variables of the foot force. Then find the optimal solution out among those with quadratic programming and friction cone constraints. The law is:

$$\begin{aligned} \min & (Af - d)^T S (Af - d) + f^T W f \\ \text{s.t.} & \|f_\tau\| < \mu \|f_n\|, 0 \leq f \leq f_{\max} \end{aligned} \quad (7)$$

where $S^{6 \times 6}$ is the optimization weight coefficient, and $W^{12 \times 12}$ is the weight of energy consumption.

As the mass of the leg is light enough to be ignored, the joint torque can be obtained by statics:

$$\tau = J_i^T {}^W_B R^T f_i, i = \{1, 2, 3, 4\} \quad (8)$$

4.2. The Model of the Swing Phase

The swing of legs is mainly to make the foot reach the desired foothold, and choice of foothold locations will affect the speed and stability of the robot. To make sure that the two successive positions can be symmetrical about the vertical projection of the hip when the foot falls, footholds follow the law below:

$$\begin{bmatrix} P_{sx} \\ P_{sy} \end{bmatrix} = \begin{bmatrix} P_{Hx} \\ P_{Hy} \end{bmatrix} + \frac{T_{st}}{2} \begin{bmatrix} v_{cx,d} \\ v_{cy,d} \end{bmatrix} + \left(\frac{g}{h}\right)^{1/2} \begin{bmatrix} v_{cx} - v_{cx,d} \\ v_{cy} - v_{cy,d} \end{bmatrix} \quad (9)$$

where $[v_{cx,d}, v_{cy,d}]^T$ is the desired velocity of the torso, T_{st} is the lasting time in stance phase, $[P_{Hx}, P_{Hy}]^T$ is the position of the vertical projection point of the intersection of the hip joint axis and the thigh link on the ground. Then we can obtain all the desired foothold locations $p_f = [p_{f,x}, p_{f,y}, p_{f,z}]^T$ in the entire swing phase by interpolating the swing trajectory with a polynomial function. Then we can calculate the virtual torque of the joint with the spring damping virtual model as:

$$\tau = k_{sp}(\theta_d - \theta) + k_{sd}(\dot{\theta}_d - \dot{\theta}) \quad (10)$$

Where $k_{sp}^{3 \times 3}$ is the stiffness coefficient and $k_{sd}^{3 \times 3}$ is the damping coefficient.

5. Simulation

First, establish MATLAB-Adams virtual prototype. The terrain established in this paper is a slope with multiple inclinations, which are 5° , 10° , 15° and 20° successively, and the horizontal length of each slope is 1.25 m. In the experiments, the desired height of the body is $H = 0.35m$, and the desired speed is $v_d = 0.3m/s$, the cycle time of the swing phase is $T_{sw} = 0.4s$, the cycle time of the stance phase is $T_{st} = 0.4s$, and the control frequency is 500 Hz. At the initial moment, the robot walks on a flat terrain with the diagonal gait and accelerates forward, then climbs up the slope later, as shown in Figure 6.

5.1. Terrain for the Torso Posture

In the simulation, the roll of the terrain should be zero. But the estimated roll is zero approximately with small fluctuation range on slopes. When the robot climbs to the next slope, the estimated roll fluctuates greatly, especially when climbing from the 20° slope to the top plane with the corresponding fluctuation is up to 4.5° , but others 1° around. Thus, the roll angle is more sensitive to terrain changes in Figure 7.

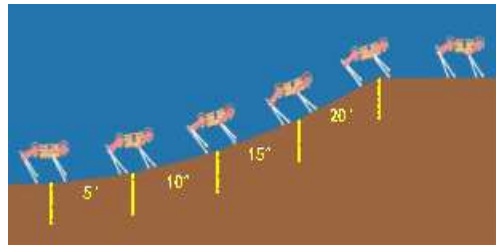


Figure 6. The simulation environment.

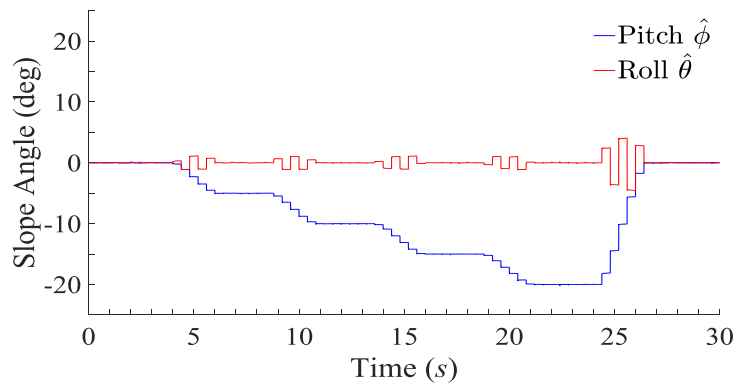


Figure 7. The pitch and roll of the estimated terrain.

5.2. Terrain for Swing Trajectory

The swing trajectory planning needs to combine the terrain information about the desired foothold utilizing the optimal method in Section 3. In Figure 8 and 9, the blue line (optimized point) indicates the estimated terrain information and the red line (latest point) is the information assigned to legs.

It can be seen from Figure 8 that the effect of estimating the terrain pitch angle by the two methods is basically the same, except that there is a slight difference in the transition phase of the slopes. Figure 9 reflects the obvious difference between the two estimated roll angles. The first method estimates a maximum fluctuation error of 5°, and the second is 3°. Overall, the second will reduce the error by 20% -70% compared to the first, and will be more beneficial to the stability of the robot.

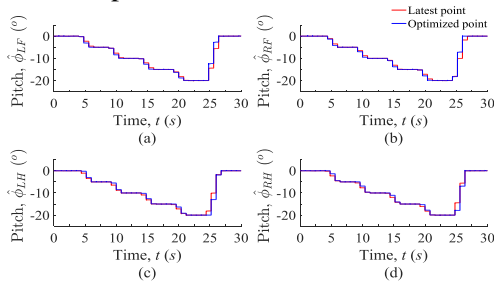


Figure 8. The pitch of the estimated terrain.

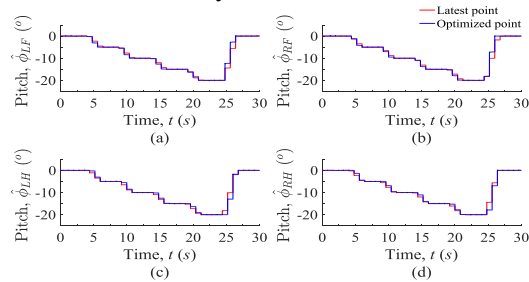


Figure 9. The row of the estimated terrain.

5.3. The Movement State of the Base

The robot realizes the stable locomotion on slopes through terrain estimation and corresponding control strategies. Figure 10 shows the velocity of the CoM while walking, where the blue line (reference) represents the desired value and the red line (actual) represents the actual value. The first picture in Figure 10 shows that the robot walks on flat ground and accelerates forward, and then the average speed reaches 0.278 m/s after a constant speed. When the robot has climbed on slopes already, the forward speed decreases by 0.008 m/s with the slope increasing 5°. The second shows the lateral velocity. With the terrain steeper, the velocity fluctuation in the Y direction of the base will increase, up to 0.03 m/s.

The third shows the vertical velocity which fluctuates periodically around 0° , and the amplitude is about 0.02 m/s, and the maximum is about 0.05 m/s.

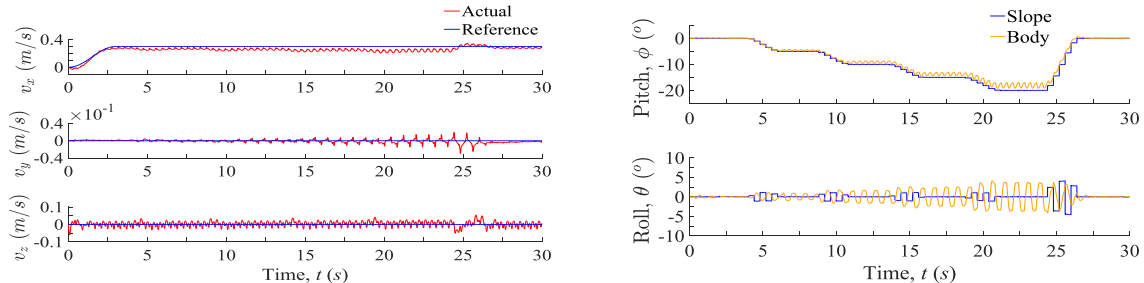


Figure 10. The velocity of the *CoM*. **Figure 11.** The pitch and roll angle of the base.

Figure 11 shows the change of the body's orientation over time, where the blue line (slope) represents the desired value, namely the estimated terrain, and the yellow (body) is the actual value. The first picture in Figure 11 shows the row angle of the base, from which we can know that the actual pitch angle will track the desired angle. But with the slope steeper, the tracking ability will be weaker and the fluctuation will be stronger. When the desired pitch angle is 20° , the average tracking error will reach 1.5° , and the fluctuation amplitude is about 1° . The second shows the roll angle of the base which fluctuates up and down around 0° , and the amplitude will be larger as the slope get steeper. When the robot is on slope of 20° , the error will reach $\pm 4^\circ$.

6. Conclusion

To make the quadruped robot walk stably, this paper proposes a method of motion on slopes based on the estimated terrain, and it is carried out the simulation test successfully. The robot can estimate the macro and the partial terrain separately, and make the corresponding adjustments. This method can make the robot walk on different slopes and transit between different terrains.

7. References

- [1] Raibert M, Blankespoor K, Nelson G and Playter R. 2008 BigDog, the Rough-Terrain Quadruped Robot. *World Congress*.
- [2] Park H. W, Park S and Kim S. 2015 Variable-speed quadrupedal bounding using impulse planning: untethered high-speed 3d running of mit cheetah 2. *IEEE*.
- [3] Semini C, Tsagarakis N G, Guglielmino E, Focchi M, Cannella F and Caldwell D G. 2011. Design of hyq – a hydraulically and electrically actuated quadruped robot. *Proceedings of the Institution of Mechanical Engineers, Part I: Journal of Systems and Control Engineering*.
- [4] Zhang X, and Zheng H. 2008 Walking up and down hill with a biologically-inspired postural reflex in a quadrupedal robot. *Autonomous Robots*, **25(1-2)**, 15-24.
- [5] Winkler A, Havoutis I, Bazeille S, Ortiz J and Semini C. 2014. Path planning with force-based foothold adaptation and virtual model control for torque controlled quadruped robots. *IEEE International Conference on Robotics & Automation*. IEEE.
- [6] Gehring C, Coros S, Hutter M, Bloesch M and Siegwart R. 2013 Control of Dynamic Gaits for a Quadrupedal Robot. *IEEE International Conference on Robotics & Automation*. IEEE.
- [7] Lee D V, Stakebake E F, Walter R M and Carrier D R. 2004 Effects of mass distribution on the mechanics of level trotting in dogs. *Journal of Experimental Biology*, **207**(Pt 10), pp 1715-1728.
- [8] Roennau A, Heppner G, Nowicki M, Zöllner JM and Dillmann R. 2014 Reactive posture behaviors for stable legged locomotion over steep inclines and large obstacles. *IEEE/RSJ International Conference on Intelligent Robots & Systems*. IEEE.
- [9] Gehring C, Bellicoso CD, Coros S, Bloesch M and Siegwart R. 2015 Dynamic trotting on slopes for quadrupedal robots. *IEEE/RSJ International Conference on Intelligent Robots & Systems*. IEEE.

- [10] Fukuoka Y, Kimura H and Cohen A.H. 2003 Adaptive dynamic walking of a quadruped robot on irregular terrain based on biological concepts. *International Journal of Robotics Research*, **26(3-4)**, pp 475-490.
- [11] Belter D and Skrzypczynski P. 2011 Rough terrain mapping and classification for foothold selection in a walking robot. *Journal of robotic systems*, **28(4)**, pp 497-528.
- [12] Bledt G, Powell M. J, Katz B, Carlo J. D, Wensing P. M and Kim S. 2019 MIT Cheetah 3: Design and Control of a Robust, Dynamic Quadruped Robot. *2018 IEEE/RSJ International Conference on Intelligent Robots and Systems (IROS)*. IEEE.
- [13] Righetti L, Buchli J, Mistry M and Schaal S. 2011 Control of legged robots with optimal distribution of contact forces. *11th IEEE-RAS International Conference on Humanoid Robots (Humanoids 2011), Bled, Slovenia, October 26-28, 2011*. IEEE.